Hepatitis C virus modulates signal peptide peptidase to alter host protein processing

Junki Hirano[a], Sachiyo Yoshio[b], Yusuke Sakai[c], Li Songling[d], Tatsuya Suzuki[a], Yumi Itoh[a], He Zhang[a], David Virya Chen[a], Saori Haga[a], Hiroko Oomori[e], Takahiro Kodama[f], Yusuke Maeda[g,h], Yoshihiro Ono[i], Yu Takahashi[i], Daron M. Standley[d,h], Masahiro Yamamoto[h,j], Kohji Moriishi[k], Kyoji Moriya[l], Tatsuya Kanto[b], Tetsuo Takehara[f], Kazuhiko Koike[l], Yoshiharu Matsuura[g,h,1], and Toru Okamoto[a,h,1]

[a]Institute for Advanced Co-Creation Studies, Osaka University, Osaka, 565-0871, Japan; [b]The Research Center for Hepatitis and Immunology, National Center for Global Health and Medicine, Chiba, 272-8516, Japan; [c]Department of Veterinary Pathology, Yamaguchi University, Yamaguchi, 753-8515, Japan; [d]Department of Genome Informatics, Osaka University, Osaka, 565-0871, Japan; [e]Core Instrumentation Facility, Osaka University, Osaka, Japan; [f]Department of Gastroenterology and Hepatology, Graduate School of Medicine, Osaka University, Osaka, Japan; [g]Department of Molecular Virology, Research Institute for Microbial Diseases, Osaka University, Osaka, 565-0871, Japan; [h]Center for Infectious Disease Education and Research, Osaka University, Osaka, 565-0871, Japan; [i]Department of Hepato-Pancreatic-Biliary Surgery, Japanese Foundation for Cancer Research, Tokyo, 135-8550, Japan; [j]Department of Immunoparasitology, Osaka University, Osaka, 565-0871, Japan; [k]Department of Microbiology, Faculty of Medicine, University of Yamanashi, Yamanashi, 409-3898, Japan; and [l]Department of Gastroenterology, Graduate School of Medicine, The University of Tokyo, Tokyo, 113-8655, Japan

Immunoevasins are viral proteins that prevent antigen presentation on major histocompatibility complex (MHC) class I, thus evading host immune recognition. Hepatitis C virus (HCV) evades immune surveillance to induce chronic infection; however, how HCV-infected hepatocytes affect immune cells and evade immune recognition remains unclear. Herein, we demonstrate that HCV core protein functions as an immunoevasin. Its expression interfered with the maturation of MHC class I molecules catalyzed by the signal peptide peptidase (SPP) and induced their degradation via HMG-CoA reductase degradation 1 homolog, thereby impairing antigen presentation to CD8+ T cells. The expression of MHC class I in the livers of HCV core transgenic mice and chronic hepatitis C patients was impaired but was restored in patients achieving sustained virological response. Finally, we show that the human cytomegalovirus US2 protein, possessing a transmembrane region structurally similar to the HCV core protein, targets SPP to impair MHC class I molecule expression. Thus, SPP represents a potential target for the impairment of MHC class I molecules by DNA and RNA viruses.

HCV | MHC class I | signal peptide peptidase | antigen presentation

Hepatitis C virus (HCV) infection is strongly associated with the development of liver steatosis, cirrhosis, hepatocellular carcinoma (HCC) (1), and extrahepatic manifestations, such as type 2 diabetes, mixed cryoglobulinemia, and non-Hodgkin lymphoma (2). Approximately 80% of patients with HCV develop chronic infections, whereas only 5% of those infected with hepatitis B virus acquire chronic infections (3). Although immune cells (i.e., T cells, NK cells, and dendritic cells) have been shown to be functionally impaired in patients with chronic hepatitis C (CHC) (4), how HCV-infected hepatocytes affect immune cells remains unclear.

In CHC patients, the administration of direct-acting antivirals dramatically improves sustained virological response (SVR) (5); however, liver disease is not ameliorated due to prolonged liver damage (6). In addition, the elimination of HCV does not fully restore immune cell proliferation and function (7, 8), suggesting that liver damage caused by HCV infection may affect the restoration of immune cell function. Thus, the characterization of viral and host factors involved in immune modulation during HCV infection is necessary to decrease the risk of HCC development in CHC patients after achieving SVR.

HCV belongs to the genus *Hepacivirus* (family *Flaviviridae*) and harbors a positive-sense, single-stranded RNA genome; its viral RNA is translated into a single polyprotein of ~3,000 amino acids that is subsequently processed into 10 viral proteins through cleavage by host and viral proteases (9). The core protein is the first to be translated and cleaved off the polyprotein by host signal peptidase. The signal sequence in the C-terminal region of the immature core protein is further processed by the host protease, signal peptide peptidase (SPP), before maturation (10). We previously demonstrated that SPP is essential for stable expression of the core protein (Fig. 1A, *Upper*). Moreover, we reported that SPP inhibition induces proteasome-dependent degradation of the core protein, mediated by an E3 ligase, a 3:8 chromosomal translocation in hereditary renal cancer (TRC8) (11) (Fig. 1A, *Lower*), and efficiently suppresses production of infectious HCV particles (12). SPP has also been reported to cleave cellular proteins, such as human leukocyte antigen-A (HLA-A), heme oxygen-1 (HO-1), X-box binding protein 1u (XBP1u), and prolactin (13–16). However, the biological significance of these cleavage events is not fully understood.

Several viruses possess immunoevasins to inhibit antigen presentation on MHC class I molecules. For instance, the Epstein–Barr virus encoding nuclear antigen 1 inhibits antigen presentation on MHC class I molecules via a Glycine–Alanine repeat (17, 18). The herpes simplex virus (HSV) encoding ICP47 and the human cytomegalovirus (HCMV) encoding US6 modulate TAP functions

Significance

The mechanism by which hepatitis C virus (HCV) evades immune surveillance and causes chronic infection is unclear. We demonstrate here that HCV core protein interferes with the maturation of major histocompatibility complex (MHC) class I catalyzed by signal peptide peptidase (SPP) and induces degradation via HMG-CoA reductase degradation 1 homolog. In addition, we found that the core protein transmembrane domain is homologous to the human cytomegalovirus US2 protein, whose transmembrane region also targets SPP to impair MHC class I molecule expression in a similar manner. Therefore, our data suggest that SPP represents a potential target for the impairment of MHC class I molecules by DNA and RNA viruses.
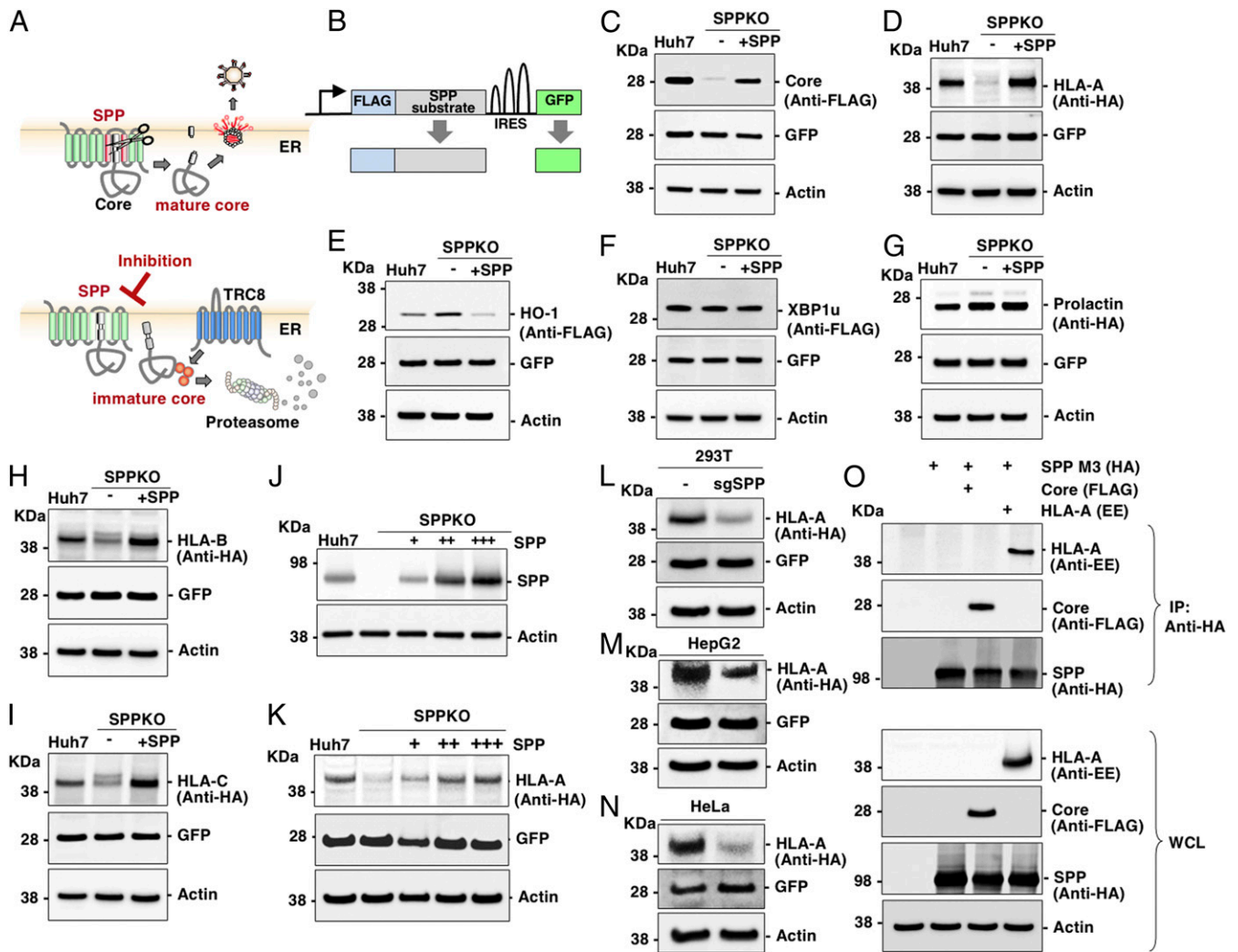
Fig. 1. SPP is essential for the stable expression of MHC I molecules. (*A*) Schematic representation of the maturation steps (*Upper*) and the degradation pathway (*Lower*) of the HCV core protein. (*B*) The structure of the bicistronic vector used. (*C*–*G*) WT, SPPKO, and SPPKO Huh7 cells expressing SPP were lentivirally transduced with the core protein (*C*), HLA-A (*D*), HO-1 (*E*), XBP1u (*F*), and prolactin (*G*). (*H* and *I*) Lentiviral vectors encoding HLA-B (*H*) or HLA-C (*I*) were transduced in WT, SPPKO, and SPPKO Huh7 cells expressing SPP. (*J*) SPPKO Huh7 cells were transduced with the lentivirus vector expressing SPP and SPPKO Huh7 cells exogenously expressing gradual levels of SPP were established. (*K*) SPPKO Huh7 cells expressing various concentrations of SPP were lentivirally expressed HLA-A. (*L*–*N*) WT and sgSPP HEK293T (*L*), HepG2 (*M*), and HeLa cells (*N*) were infected with the lentivirus expressing HLA-A. (*O*) HEK293T cells were transfected with HA-tagged SPP and FLAG-tagged core or EE-tagged HLA-A. The immunoprecipitated samples (IP) and whole-cell lysates (WCL) were subjected to sodium dodecyl-sulfate polyacrylamide gel electrophoresis and immunoblotting. The data shown in *C*–*O* are representative of three independent experiments.

to inhibit the translocation of antigenic peptides to the endoplasmic reticulum (ER) lumen (19–21). Adenoviruses encode E3-19K protein to retain MHC class I molecules within the ER, whereas human immunodeficiency viruses encode Nef to induce the translocation of MHC class I molecules from the trans-Golgi network to the lysosome, thereby blocking their cell surface expression (22, 23). Meanwhile, Ebola virus possesses glycoprotein that interact with MHC class I molecules expressed on the cell surface to prevent their antigen presentation via steric shielding (24). Moreover, the viral E3 ligase K3 encoded by murine γ-herpes virus and the glycoproteins US2 and US11 encoded by HCMV induce the degradation of MHC class I molecules (25–28).

HLA-A, a substrate of SPP, is a member of the classical major histocompatibility complex (MHC) class I gene family. Intracellular peptides derived from pathogens are loaded on MHC class I molecules presenting on cell surfaces and are recognized by the CD8⁺ T cells. In this study, we investigated whether SPP substrates induce degradation following SPP inhibition.

Results

SPP Is Crucial for the Expression of MHC Class I Molecules. We constructed bicistronic lentiviral vector expressing SPP substrates (Fig. 1*B*) and found that the core protein expression was suppressed in SPPKO Huh7 cells, as reported previously (Fig. 1*C*). Expression of HLA-A was reduced in SPPKO cells (Fig. 1*D*), whereas that of HO-1, XBP1u, and prolactin showed no significant difference between the wild-type (WT) and SPPKO cells (Fig. 1 *E*–*G*). Moreover, SPP deficiency did not impact the expression of other membrane proteins, such as transferrin receptor 1 (TFR1, *SI Appendix*, Fig. S1*A*). Taken together, these results suggest that HLA-A expression is dependent on SPP.

HLA-A, -B, and -C are classical MHC class I molecules, which are highly polymorphic proteins and are widely expressed in all tissues, whereas HLA-E, -F, and -G are nonclassical MHC class I molecules, which are usually nonpolymorphic proteins and show restricted expression patterns. To examine whether the expression of other MHC class I molecules is also dependent on SPP, these

molecules were expressed in SPPKO Huh7 cells. We found that expression of HLA-B and -C was impaired in SPPKO Huh7 cells (Fig. 1 *H* and *I*) but that of HLA-E, -F, and -G was not (*SI Appendix*, Fig. S1*B*). These data suggest that the expression of classical MHC class I molecules is dependent on SPP.

Next, we generated SPPKO Huh7 cells exogenously expressing gradual levels of SPP (Fig. 1*J*). The expression of HLA-A and the core protein was restored by SPP expression (Fig. 1*K* and *SI Appendix*, Fig. S1*C*). In addition, we confirmed the impaired expression of MHC class I molecules in HEK293T, HepG2, and HeLa cells expressed single-guided (sg) SPP and Cas9 (Fig. 1 *L–N* and *SI Appendix*, Fig. S1*D*). Finally, coimmunoprecipitation assay revealed that SPP specifically interacted with the core protein and HLA-A but not with TFR1 (Fig. 1*O* and *SI Appendix*, Fig. S1*E*). Collectively, our data revealed that SPP is a regulator of classical MHC class I molecules.

Proteolytic Activity of SPP Regulates the Expression of MHC Class I.
To examine the effect of SPP inhibitors (29) on the expression of HLA-A, Huh7 cells stably expressing HLA-A were treated with various concentrations of these inhibitors. Treatment with YO-01027, LY-411575, and RO-4929097 but not DAPT, which is an inactive relevant to YO-01027, efficiently suppressed HLA-A expression in a dose-dependent manner (Fig. 2*A*). In addition, YO-01027 treatment suppressed the expression of HLA-B and -C but not of HO-1, XBP-1u, and prolactin (Fig. 2*B* and *SI Appendix*, Fig. S2 *A–C*). The impairment of HLA-A expression by YO-01027 was also confirmed in HEK293T, HepG2, and HeLa cells (Fig. 2*C*). These data suggest that the inhibition of the protease activity of SPP impairs the expression of MHC class I molecules.

SPP has two putative protease active sites at Asp219 and Asp265. We found that HLA-A expression was only restored in SPPKO Huh7 cells expressing WT SPP, not those expressing the mutant variant (Fig. 2 *D* and *E*). We also examined SPPKO Huh7 cells producing immature and uncleaved HLA-A and found that HLA-A fused with FLAG and HA at the N and C terminus, respectively (FLAG-HLA-A-HA, Fig. 2*F*), was expressed in SPPKO Huh7 cells as well as in those expressing SPP. Although uncleaved HLA-A was not observed in either cell line, treatment with a proteasome inhibitor Ac-Leu-Leu-Nle-Aldehyde (ALLN) markedly restored the expression of uncleaved HLA-A in SPPKO Huh7 cells (Fig. 2*G*). These data suggest that immature HLA-A is quickly degraded by proteasomes.

We then investigated the cell surface expression of MHC class I molecules in SPPKO cells using flow cytometry. Expression of endogenous MHC class I molecules, not TFR1, was impaired in SPPKO Huh7 cells; however, it was restored by exogenous expression of SPP (Fig. 2*H* and *SI Appendix*, Fig. S2*D*). Moreover, treatment with YO-01027, not DAPT, also impaired expression of endogenous MHC class I molecules (*SI Appendix*, Fig. S2*E*). Furthermore, the stability of MHC class I molecules was impaired in SPPKO Huh7; however, it was restored via exogenous expression of SPP (Fig. 2*I*). Collectively, these data suggest that the proteolytic activity of SPP is required for the stable expression of MHC class I molecules.

The molecular mechanism underlying the degradation of immature MHC class I molecules in SPPKO cells was also elucidated. β2M is essential for stable expression of MHC class I molecules (30) (Fig. 2*J*). Moreover, we observed that β2M overexpression caused a slight enhancement of HLA-A levels in WT Huh7 cells but not in SPPKO Huh7 cells (Fig. 2*K*). Additionally, although the HLA-A messenger RNA (mRNA) levels were comparable between WT and SPPKO Huh7 cells (*SI Appendix*, Fig. S2*F*), expression of MHC class I molecules was restored by treatment with ALLN (*SI Appendix*, Fig. S2*G*). Previous studies have reported that TRC8 and HMG-CoA reductase degradation 1 homolog (HRD1)

are functional E3 ligases for MHC class I molecules (25, 31, 32). The core protein expression was clearly restored in sgTRC8/SPPKO Huh7 cells but not in sgHRD1/SPPKO Huh7 cells (Fig. 2*L*). Meanwhile, loss of HRD1 but not TRC8 in SPPKO Huh7 cells inhibited the degradation of HLA-A, -B, and -C (Fig. 2 *M* and *N*). Expression of endogenous MHC class I molecules was also restored in sgHRD1/SPPKO Huh7 cells (*SI Appendix*, Fig. S2*H*). Additionally, treatment with PNGase F, which is an enzyme to remove N-linked glycosylation, revealed that the glycosylation status of immature MHC class I molecules in SPPKO Huh7 cells was similar to that of SPPKO Huh7 cells expressing SPP (*SI Appendix*, Fig. S2*I*). Meanwhile, immunoprecipitation results showed that SPP interacted with both TRC8 and HRD1 but not with green fluorescent protein (GFP) or TFR1 (Fig. 2*O* and *SI Appendix*, Fig. S1*E* and S2*J*). Collectively, these data suggest that immature MHC class I molecules produced in SPPKO cells are recognized and that their degradation is induced by HRD1.

Considering that we have also previously shown that TRC8-mediated degradation of the immature core represents a type of ER quality control (12), we next examined the effect of immature HLA-A on ER stress. While deficiency of SPP did not contribute to the induction of ER stress (*SI Appendix*, Fig. S2*K*), the immature core protein produced in sgTRC8/SPPKO Huh7 cells but not the immature HLA-A produced in sgHRD1/SPPKO Huh7 cells induced ER stress (*SI Appendix*, Fig. S2*L*), suggesting that induction of ER stress by immature SPP substrate occurs in a substrate-specific manner.

SPP Regulates Antigen Presentation on MHC Class I Molecules. Next, we determined whether SPP deficiency functionally impairs antigen presentation on MHC class I molecules. Although IFN-γ production was dependent on the coculture with CD8$^+$ T cells and the addition of OVA peptide (Fig. 3*A* and *SI Appendix*, Fig. S2*M*), it was significantly impaired in the supernatants of SPP$^{-/-}$ mouse embryonic fibroblasts (MEFs) and CD8$^+$ T cell coculture system (Fig. 3*B*). In addition, the exogenous expression of WT SPP but not of mutant SPP restored IFN-γ production in SPP$^{-/-}$ MEFs (Fig. 3*B*). Furthermore, treatment of WT MEFs with YO-01027 but not with DAPT suppressed IFN-γ production (Fig. 3*C*). Collectively, these results suggest that proteolysis of MHC class I molecules by SPP plays a crucial role in the antigen presentation to activate CD8$^+$ T cells.

As the expression of both SPP and MHC class I molecules was impaired in liver-specific SPP-knockout mice (SPPLKO, Fig. 3 *D–F*), we sought to determine the effects of SPP deficiency on liver pathogenicity. Liver sections of 2-mo-old SPPLKO mice showed no apparent abnormality. Moreover, no obvious steatosis, macrophage, CD3$^+$T cell infiltration, or activated satellite cells was observed (Fig. 3*G*). We also confirmed that the transcriptional levels of inflammatory genes were comparable between the WT and SPPLKO mice (Fig. 3*H*). Hence, loss of SPP does not appear to impact the expression of inflammatory genes or tissue structure; however, it does impair the expression of MHC class I molecules.

HCV Core Protein Promotes the Degradation of MHC Class I Molecules. Next, we examined the involvement of the HCV core protein on MHC class I expression and found that the HCV core protein suppress HLA-A expression, whereas that of Japanese encephalitis virus, which matures independently of SPP (33), had no effect (Fig. 4 *A* and *B*). Furthermore, we observed that HCV infection significantly reduced HLA-A expression in Huh7 cells expressing HLA-A (Fig. 4*C*).

We also examined the effects of the HCV genotypes on impaired HLA-A expression. Each of the core proteins derived from the seven genotypes (GT1 to GT7) exhibited impaired HLA-A expression. Among these, the effects of core proteins derived from GT3, GT4, and GT6 were the most potent (*SI Appendix*,
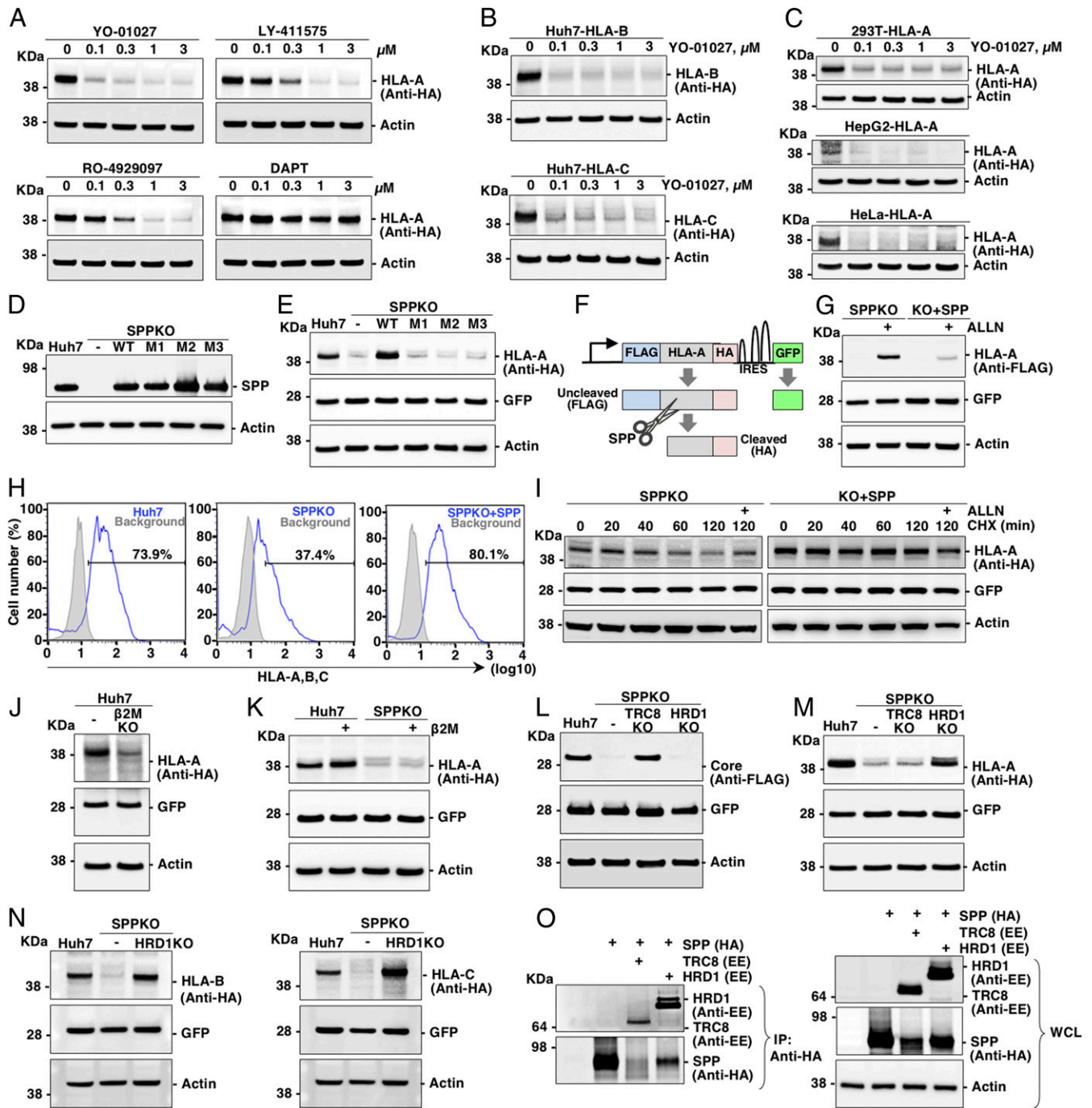
MICROBIOLOGY

Hirano et al.
Hepatitis C virus modulates signal peptide peptidase to alter host protein processing

PNAS | 3 of 12
https://doi.org/10.1073/pnas.2026184118

www.manaraa.com

Fig. 2. SPP cleavage is required for the stable expression of MHC class I molecules. (*A*) Huh7 cells stably expressing HLA-A were treated with YO-01027, LY-411575, RO-4929097, and DAPT. (*B*) Huh7 cells stably expressing HLA-B (*Upper*) or HLA-C (*Lower*) were treated with YO-01027. (*C*) HEK293T (*Upper*), HepG2 (*Middle*), and HeLa (*Lower*) cells stably expressing HLA-A were treated with YO-01027. (*D*) SPPKO Huh7 cells were infected with the lentivirus expressing HA-tagged SPP (WT), SPP D219A (mutant 1; M1), SPP D265A (mutant 2; M2), or SPP D219/D265A (mutant 3; M3). (*E*) SPPKO Huh7 cells stably expressing WT or SPP mutants were infected with the lentivirus expressing HLA-A. (*F*) Structure of the N-terminal FLAG-tagged and C-terminal HA-tagged HLA-A (FLAG-HLAA-HA) and GFP under the control of the ubiquitin promoter. (*G*) SPPKO and SPPKO Huh7 cells expressing SPP were infected with the lentivirus expressing HLA-A and treated with ALLN. (*H*) Surface expression of MHC class I molecules in WT (*Left*), SPPKO (*Middle*), and SPPKO Huh7 cells expressing SPP (*Right*) were determined using flow cytometry. (*I*) Stability of HLA-A was examined by treatment with cycloheximide (CHX) and ALLN in SPPKO (*Left*), and SPPKO Huh7 cells expressing SPP (*Right*) (*J*) WT and sgβ2M Huh7 cells and (*K*) WT and SPPKO Huh7 cells expressing β2M were infected with the lentivirus expressing HLA-A. HLA-A expression was detected using immunoblotting 48 h post-transduction using anti-HA antibodies. (*L* and *M*) The sgTRC8/SPPKO and sgHRD1/SPPKO Huh7 cells were infected with the lentivirus expressing (*L*) the core protein and (*M*) HLA-A. (*N*) The sgHRD1/SPPKO Huh7 cells were infected with lentivirus expressing HLA-B or -C. (*O*) HEK293T cells were transfected with HA-tagged SPP and Glu-Glu (EE)-tagged TRC8 or EE-tagged HRD1. The immunoprecipitated samples (IP) and whole-cell lysates (WCL) were subjected to sodium dodecyl-sulfate polyacrylamide gel electrophoresis and immunoblotting. The data shown in *A–E*, *G*, and *J–O* are representative of three independent experiments; those in *H* and *I* are representative of two independent experiments.
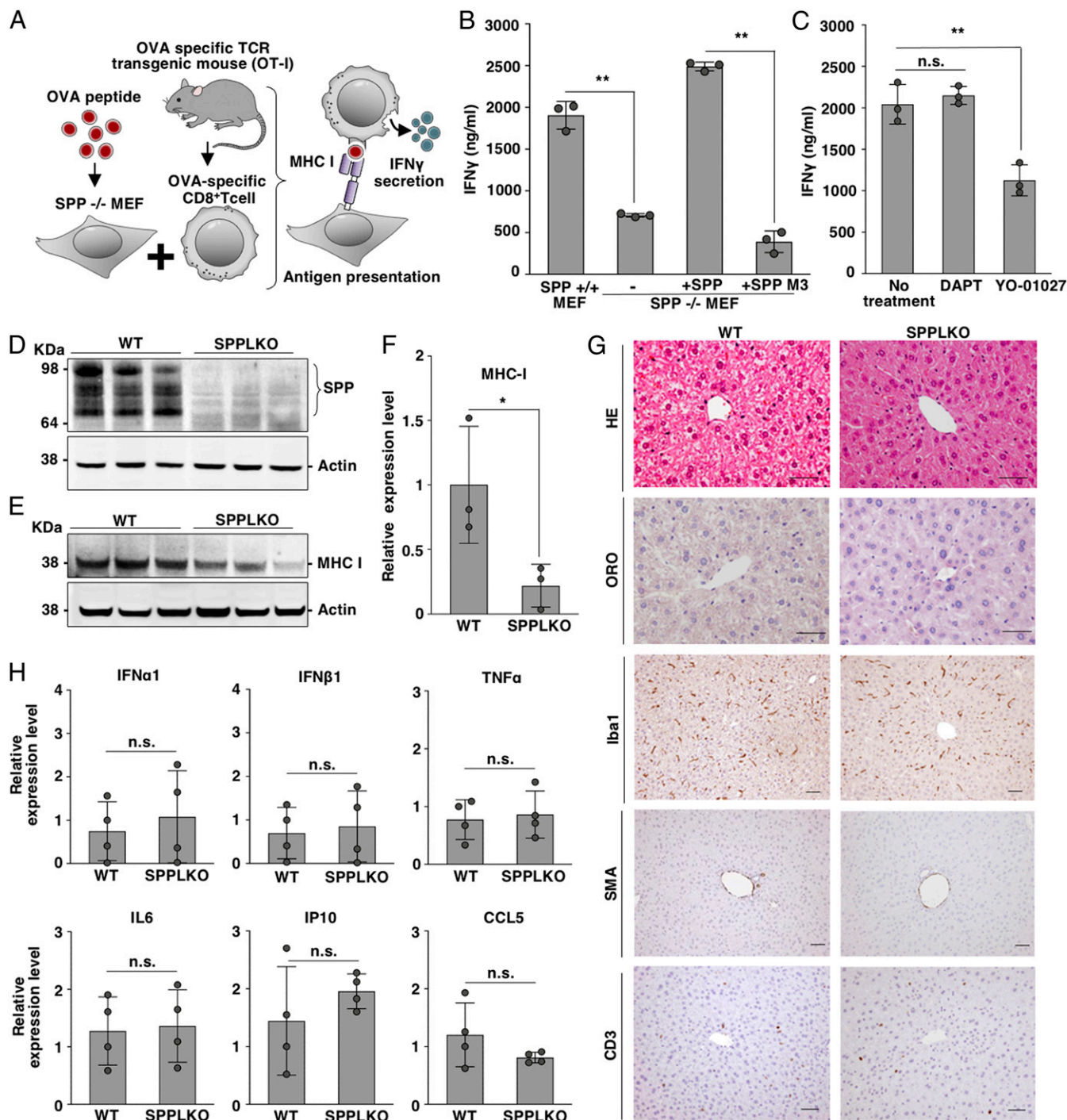
www.manaraa.com

Fig. 3. SPP is required for antigen presentation to CD8⁺ T cells. (*A*) Schematic representation of the antigen presentation assay. (*B*) SPP⁺/⁺ MEFs, SPP⁻/⁻ MEFs, SPP⁻/⁻ MEFs expressing SPP, and SPP⁻/⁻ MEFs expressing SPP D219/265A (mutant 3; M3) were treated with the OVA peptide (1.0 nM) for 7 h and cocultured with OVA-specific CD8⁺ T cells for 72 h. (*C*) SPP⁺/⁺ MEFs were treated with YO-01027 or DAPT (10 μM) for 24 h and cocultured with OVA-specific CD8⁺ T cell. (*D*) SPP expression of WT or SPPLKO male mice ($n = 3$, 2-mo old). (*E*) The liver lysates in *D* were subjected to immunoblotting, and the (*F*) signal intensities of each band were quantified. The relative expression of MHC class I molecules was normalized to that of actin. (*G*) Liver sections were stained using hematoxylin eosin (HE), oil red O (ORO), Iba1 (also named Daintain/AIF-1), CD3, and smooth muscle actin (SMA) (Scale bars, 50 μm). (*H*) mRNA levels were determined using qPCR ($n = 4$). The data are representative of two (*B* and *C*) or three (*D*–*H*) independent experiments and are presented as the mean ± SD. Significance (*$P < 0.05$; **$P < 0.01$; n.s., not significant) was determined using Student's t test ($n = 3$ in *B*, *C*, and *F*; $n = 4$ in *H*).

Fig. S3*A*). Furthermore, an experiment using cycloheximide showed that HLA-A stability was impaired by exogenous expression of the core protein (Fig. 4*D*). Next, to examine whether HLA-A was degraded by HRD1, the core protein was expressed in Huh7 or sgHRD1 Huh7 cells stably expressing HLA-A, -B, or -C. While expression of the core protein reduced the expression HLA-A, -B, and -C (Fig. 4*E*), these effects were restored by sgHRD1 transduction (Fig. 4*F*). Thus, our data suggest that the HCV core protein induces HRD1-mediated degradation of MHC class I molecules during HCV infection.
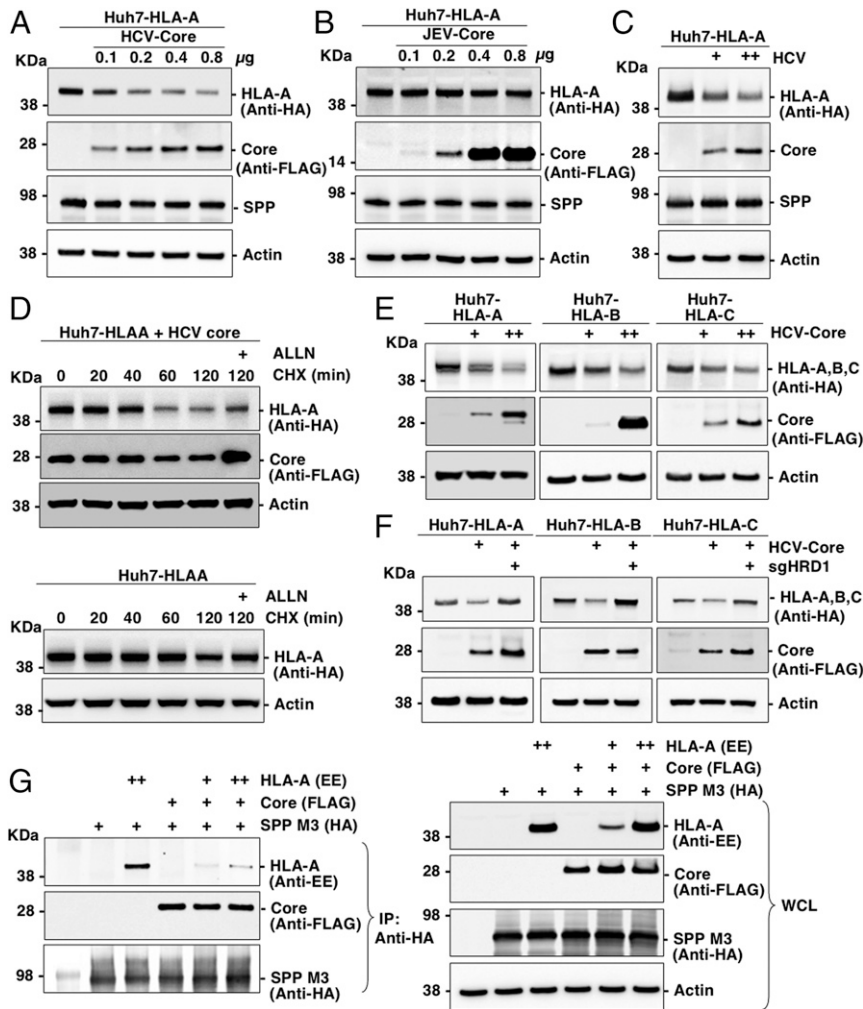
Fig. 4. Core protein impairs the interaction between SPP and MHC class I molecules and induces the degradation of MHC class I molecules. (*A* and *B*) Huh7 cells stably expressing HLA-A were transfected with 0.1, 0.2, 0.4, or 0.8 μg of the (*A*) pCAG OSF-HCV or (*B*) pCAG FLAG-JEV core. (*C*) Huh7 cells stably expressing HLA-A were infected with HCV at a multiplicity of infection of 5.0 or 10.0 and incubated for 96 h. (*D*) Huh7 cells stably expressing HLA-A were transduced with the core protein. Stability of HLA-A was evaluated by treatment with cycloheximide (CHX) and ALLN. (*E*) Huh7 cells stably expressing HLA-A (*Left*), HLA-B (*Middle*), and HLA-C (*Right*) were transfected with pCAG OSF-HCV core. (*F*) The WT or sgHRD1 Huh7 cells stably expressing HLA-A (*Left*), HLA-B (*Middle*), and HLA-C (*Right*) were transfected with pCAG OSF-HCV core. (*G*) HEK293T cells were transfected with HLA-A-EE, FLAG-core, and SPP-HA D219/265A (M3). The immunoprecipitated samples (IP) and whole-cell lysates (WCL) were subjected to sodium dodecyl-sulfate polyacrylamide gel electrophoresis and immunoblotting. The data are representative of three independent experiments.

Lastly, we investigated how the core protein induces MHC class I molecule degradation. Immunoprecipitation analysis revealed that SPP could specifically interact with HLA-A and the core protein (Figs. 1*O* and 4*G*; lanes 3 and 4), while interactions between SPP and HLA-A was impaired by the interaction between SPP and the core protein (Fig. 4*G*, lanes 5 and 6), indicating that the core protein suppressed the interaction between SPP and MHC class I molecules. In addition, expression of the core protein produced uncleaved HLA-A as shown in Fig. 2*F* (*SI Appendix*, Fig. S3*B*). Taken together, our data suggest that the core protein directly binds to SPP and attenuates SPP activity, thus producing immature MHC class I molecules and inducing HRD1-mediated degradation. Because SPP is expected to have other substrates in addition to those we tested in Fig. 1, we speculate that the HCV-core–mediated modulation of SPP activity may globally alter protein processing.

HCV Core Protein Antagonizes the MHC Class I Antigen Presentation Machinery. We found that the expression of endogenous MHC class I molecules but not TFR1 was down-regulated by the

expression of core protein (Fig. 5*A* and *SI Appendix*, Fig. S3*C*). Moreover, IFN-γ produced by the CD8^{+} T cells cocultured with MEFs expressing the core protein was significantly decreased compared with those cultured with MEFs expressing GFP (Fig. 5*B*). In the livers of CoreTg mice, the expression of MHC I class I molecules was significantly impaired (Fig. 5 *C* and *D*).

Consistent with the MEF results, IFN-γ production by CD8^{+} T cells cocultured with the hepatocytes of CoreTg mice was significantly impaired compared with that of WT mice (Fig. 5*E*). We next investigated the liver samples of CHC patients who underwent surgical resection. Similar to the results described above, expression of MHC class I molecules in the livers of CHC patients was significantly impaired compared with normal livers (Fig. 5*F*), while core protein levels did not correlate with that of MHC class I molecules. Next, we examined the effects of HCV elimination on the expression of MHC class I molecules in the livers of CHC patients and other hepatic diseases. Although the expression of MHC class I molecules in the SVR group was slightly higher compared to that of the control group, no statistically significant differences were observed between this group (Fig. 5*G*) and the control and

www.manaraa.com

nontumor tissues of those with nonalcoholic steatohepatitis or alcoholic hepatitis (Fig. 5*H*). Collectively, these data suggest that HCV infection specifically impaired the expression of MHC class I molecules thereby evading immune system recognition, which might be associated with the promotion of viral survival.

SPP Is a Common Target for the Down-Regulation of MHC Class I Molecules by Viruses. SPP has been suggested to interact with the HCMV-encoded US2 protein and is involved in the degradation of MHC class I molecules (34). Therefore, we compared the roles of HCMV US2 and the HCV core protein in the down-regulation of MHC class I molecules. Results show that HLA-A expression was significantly decreased following US2 expression (Fig. 6 *A* and *B*). Immunoprecipitation results further revealed that SPP with mutated protease active sites exhibited enhanced interaction with US2 compared with WT SPP (Fig. 6*C*), suggesting that the proteolytic activity of SPP participates in the interaction between US2 and SPP. Moreover, alignment using HHpred revealed that the transmembrane region of HCV core protein was partially shared with that of US2 (Fig. 6*D*). In addition, in silico modeling of HCV core protein and HCMV US2 revealed similar helix structure, suggesting that US2 is a potential target of SPP (Fig. 6*E*). To determine whether US2 is a substrate of SPP, US2 fused with HA and FLAG at the N and C terminus, respectively (Fig. 6*F*), was expressed in HEK293T cells and treated with YO-01027. Although the molecular size of US2 showed no change following YO-01027 treatment (Fig. 6*G*), that of the HCV core protein was higher. In addition, uncleaved HCV core protein was detected by YO-01027 treatment (Fig. 6*H*). These data suggest that US2 is not cleaved by SPP. In US2-expressing Huh7 cells, we observed severely impaired expression of the mature HLA-A detected by the anti-HA antibody, and ALLN treatment enhanced the expression of immature HLA-A detected (Figs. 2*F* and 6*I*). These data suggest that US2 expression inhibited the cleavage of HLA-A by SPP.

Next, we examined whether US2-mediated HLA-A degradation is dependent on TRC8 or HRD1. HLA-A expression was restored in sgTRC8 Huh7 cells (Fig. 6*J*), suggesting that US2 expression induced the TRC8-dependent HLA-A degradation as previously reported (25). Furthermore, immunoprecipitation results revealed that SPP interacted with TRC8 and US2 (*SI Appendix*, Fig. S3*D*). In contrast to the core protein, US2 expression did not affect the interaction between SPP and HLA-A (Fig. 6*K*). This indicates that the HCV core, as well as HCMV-derived US2, target SPP for the degradation of MHC class I molecules, albeit with different molecular mechanisms.

Overall, we demonstrated the viral strategies, utilizing SPP, for the down-regulation of MHC class I molecules. HCMV US2 interacts with SPP to inhibit the maturation of MHC class I molecules via SPP inhibition, thereby inducing TRC8-dependent degradation without cleavage by SPP (Fig. 6*L*). Meanwhile, HCV core protein interacts with SPP and inhibits the maturation of MHC class I molecules through cleavage by SPP, thus inducing HRD1-dependent degradation (Fig. 6*M*). These two viruses utilize SPP to down-regulate MHC I molecules and evade immune recognition by CD8$^+$ T cells (Fig. 6*N*).

Discussion

SPP cleaves the core proteins of viruses belonging to the genera *Pestivirus* and *Hepacivirus* and is critical for core protein maturation. We have previously demonstrated its key role in the formation of infectious particles and liver pathogenesis of HCV (12, 29). Although SPP cleaves cellular proteins (13–16), to the best of our knowledge, there is no report on its role in the expression of cellular substrates. Therefore, we investigated whether other SPP substrates also undergo degradation due to SPP inhibition. We also examined whether the expression of the core protein interferes with their maturation.

Among the SPP substrates, MHC class I molecules, namely HLA-A, -B, and -C but not -E, -F, and -G, were degraded by SPP inhibition, indicating that SPP is essential for the maturation of classical MHC class I molecules. HLA-A, -B, and -C are reportedly cleaved by SPP, the cleaved products are then loaded on HLA-E and play a role in "self" recognition by immune cells, such as NK cells (13). We further showed that SPP inhibition induces the HRD1-mediated degradation of classical MHC class I molecules and that SPP is important for antigen presentation to CD8$^+$ T cells. Once the signal peptides of the N terminus of HLAs are cleaved by the signal peptidase, mature HLAs can be produced before cleavage by SPP. However, it remains unclear as to why the signal peptide cleaved by SPP is critical for HLA maturation. Although this peptide is loaded on HLA-E for "self" recognition to inhibit NK cells, our data suggest that it also stabilizes mature MHC class I molecules.

The expression of mature MHC class I molecules is tightly regulated at the transcriptional and post-translational levels. For example, the binding immunoglobulin protein, calnexin, calreticulin, and the protein disulfide isomerase family A member 3 are required for MHC class I expression (35–38). In addition, the interaction between MHC class I molecules and β2M is essential for subsequent formation of the peptide-loading complex, comprising a transporter associated with antigen processing (TAP) and Tapasin (39). In this study, we have revealed that the catalytic cleavage by SPP is required for the expression of MHC class I molecules.

The degradation of MHC class I molecules has been extensively studied. Cells lacking β2M induce the HRD1-dependent degradation of MHC I molecules (31, 40). Furthermore, the HLA-B27 of MHC class I molecules is strongly associated with ankylosing spondylitis (41). HLA-B27 is prone to induce its misfolding, resulting in its degradation (42). In addition, the homeostatic iron regulator (*HFE*) is also a member of the MHC class I protein family. The *HFE* containing the Cys282 mutation to Thy (HFE-C282Y) has impaired surface expression and is strongly associated with the development of hereditary hemochromatosis (43). Interestingly, both the HLA-B27 and HFE-C282Y are degraded by HRD1 (31). Although it remains unclear whether the machinery for HRD1-mediated degradation is similar to that of HLA-A, -B, and -C (i.e., via SPP inhibition) we revealed that immature MHC class I molecules produced via SPP inhibition utilized HRD1 as a ubiquitin ligase similar to HLA-B27 and HEF-C282Y. The pathological consequences of the down-regulation of classical MHC class I molecules by SPP inhibition should be explored in future studies.

Our data indicated that the HCV core protein inhibited the cleavage of MHC class I molecules and induced their degradation similar to US2, thus strongly suggesting that the core protein functions as an immunoevasin. US2, a glycoprotein possessing a type I transmembrane domain, interacts with SPP (34) and induces the TRC8-dependent degradation of MHC class I molecules (25). We revealed that the active sites of SPP are involved in interaction with US2, while US2 inhibits the proteolysis of MHC class I molecules to induce TRC8-dependent degradation. Although it remains unclear how the tertiary complex of SPP, MHC class I molecules, and US2 or the core protein is formed at the ER, SPP may be a suitable target for the suppression of MHC class I molecules in DNA and RNA viruses. Moreover, the core protein modulates other SPP substrates, which might be involved in other cellular functions, such as HCV-induced liver pathogenesis.

In addition, SPP cleaves the viral proteins of the Bunyamwera virus and HSV (glycoprotein K) (44–46) and plays an important role in their propagation. Therefore, the biological significance of using the host SPP in these viruses should be further investigated. *Pestivirus* and *Hepacivirus* utilize SPP for the maturation of the core protein. Interestingly, the expression of MHC class I
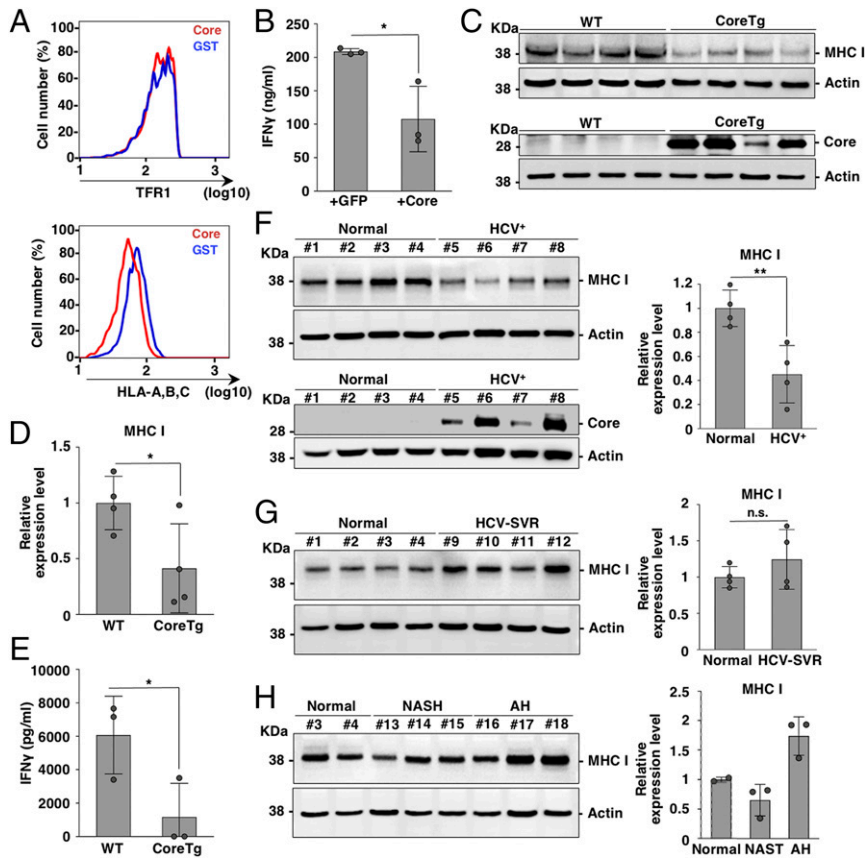
Fig. 5. Core protein impairs antigen presentation on MHC I molecules. (*A*) Endogenous expression of TFR1 (*Upper*) or HLA-A, -B, and -C (*Lower*) in Huh7 cells expressing glutathione S-transferase (GST) or the core protein was analyzed using flow cytometry. (*B*) The WT MEFs expressing GFP or the core protein were treated with OVA peptides (1.0 nM) and cocultured with OVA-specific CD8$^+$ T cells for 72 h. (*C*) Liver lysates from WT and CoreTg male mice ($n = 4$, 2-mo old) and (*D*) the expression of MHC class I molecules. (*E*) Hepatocytes derived from WT or CoreTg mice were treated with OVA peptides and cocultured with OVA-specific CD8$^+$ T cells. (*F*) Nontumor samples from normal livers (normal) and HCV-positive livers (HCV$^+$) ($n = 4$). Quantification of the expression of MHC class I molecules (*Left*) and their normalization (*Right*). (*G*) Nontumor samples from normal livers (normal) and livers of SVR patients (HCV-SVR) ($n = 4$; *Left*). (*H*) Nontumor samples from normal livers (normal) and livers of patients with nonalcoholic steatohepatitis (NASH) or alcoholic hepatitis (AH) ($n = 3$; *Left*). IFN-γ levels were determined using enzyme-linked immunosorbent assay. Liver lysates were subjected to immunoblotting, and the expression of MHC class I molecules was quantified and normalized to that of actin. The data are representative of two independent experiments and are presented as the mean ± SD shown in ($n = 3$ in *B*, *E*, and *H*; $n = 4$ in *D* and *F*–*H*. Significance (*$P < 0.05$; **$P < 0.01$; n.s., not significant) was determined using Student's *t* test.

molecules was reduced in cells infected with bovine diarrhea virus and border disease virus (47, 48). Thus, the core protein has been proposed to play a key role in the impairment of the MHC class I expression in cells infected with *Pestivirus*. Further studies are warranted to identify the virus-specific differences in the maturation between the core protein by SPP and the viral protease in the *Flaviviridae* family.

The down-regulation of MHC class I molecules by SPP inhibition or the expression of the core protein might impair "self" recognition and activate NK cells. We demonstrated that the degradation of classical MHC class I molecules was induced in SPPKO cells and core-expressing cells. NKG2D is a major activating receptor expressed in NK cells and recognizes the MHC class I polypeptide–related sequence A, MHC class I polypeptide–related sequence B, and ULBP1-6 rather than the classical MHC class I molecules in humans (49). The heterodimer of CD94 and NKG2A of NK cells recognizes HLA-E to inhibit the activation of NK cells (49). Therefore, not only classical MHC class I molecules but also other molecules (i.e., nonclassical MHC class I molecules) participate in the regulation of NK cells. We observed that the livers of SPPLKO mice did not exhibit inflammation. Moreover, those of β2M$^{-/-}$ mice, which lack the cell surface expression of MHC class I molecules, exhibited no inflammation (50). Although some of the nonclassical MHC class I

molecules can mature independently of β2M, how SPP contributes to the regulation of NK cells requires further investigation.

In summary, we showed that SPP is required for the stable expression of MHC class I molecules and that their catalytic cleavage by SPP is crucial for antigen presentation to, and subsequent recognition by, CD8$^+$ T cells. We also demonstrated how the HCV core protein evades antigen presentation on MHC class I molecules; particularly, SPP inhibition and the expression of the core protein induced the HRD-1–dependent degradation of MHC class I molecules. Finally, we confirmed the impairment of MHC class I molecules in CoreTg mice and patients infected with HCV. Our findings illustrate an immune evasion strategy of HCV to avoid recognition by host (*SI Appendix*, Fig. S4). Specifically, the core protein was found to interfere with the interaction between SPP and HLA-A, thereby inducing accumulation of immature HLAs and subsequent HRD1-dependent degradation by proteasomes.

Materials and Methods

Cell Lines and Virus. Human hepatoma cell lines (i.e., Huh7, Huh7.5.1, and HepG2), human embryonic kidney cell line (HEK293T), and HeLa cells derived from cervical carcinoma cells were obtained from the National Institute of Infectious Disease. MEFs were generated from E14.5 embryos as described previously (12). The SPP, TRC8, and SPP/TRC8 knockout Huh7 cells and MEFs were previously described (12). All cell lines were maintained in Dulbecco's modified Eagle's medium supplemented with 10% fetal bovine serum (FBS),
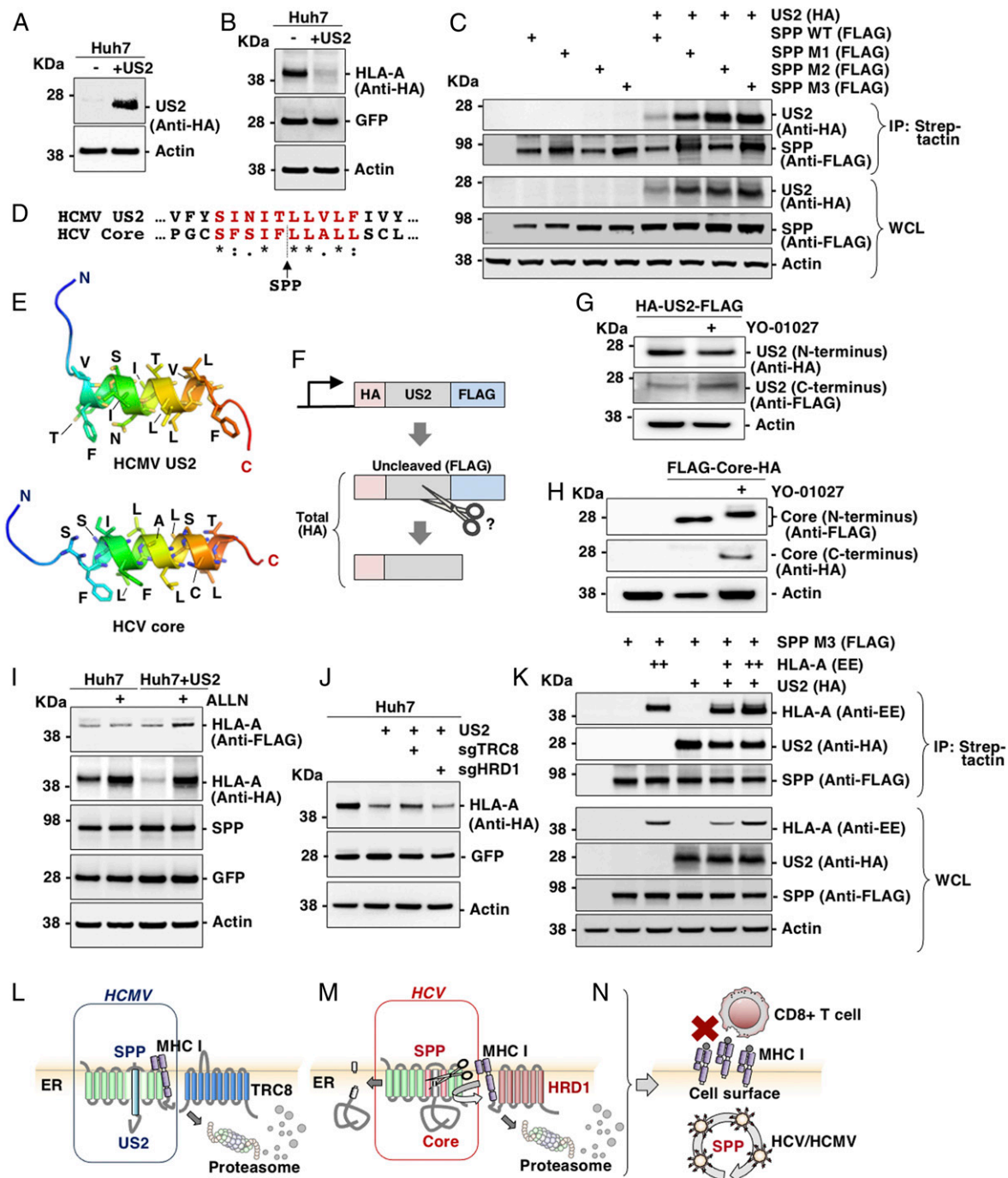
www.manaraa.com

Fig. 6. The HCV core protein and the HCMV-derived US2 protein target SPP to down-regulate MHC class I molecules. (*A*) Huh7 cells were transduced with the lentivirus vector expressing US2. (*B*) Huh7 cells and Huh7 cells stably expressing US2 were infected with the lentivirus expressing HLA-A. (*C*) HEK293T cells were transfected with HA-US2 and FOS-tagged SPP (WT), SPP-FOS D219A (M1), SPP-FOS D265A (M2), or SPP-FOS D219/265A (M3). The immunoprecipitated samples (IP) and whole-cell lysates (WCL) were subjected to sodium dodecyl-sulfate polyacrylamide gel electrophoresis and immunoblotting. (*D*) Comparison of the amino acids in the transmembrane domain of US2 and the core protein. Amino acids predicted as a homolog by HHpred are indicated in red; the cleavage site of the core protein by SPP is indicated by the arrow. (*E*) Homology modeling of the HCMV US2 (*Upper*) and the HCV core protein (*Lower*) was conducted using MODELER. Each helix structure is illustrated, and the side chains of the helix regions are represented by sticks. (*F*) Structure of the US2-tagged HA and FLAG in the N and C terminus, respectively (HA-US2-FLAG). (*G* and *H*) HEK293T cells were transfected with (*G*) US2 and (*H*) the core protein and treated with YO-01027. (*I*) SPPKO and SPPKO Huh7 cells expressing SPP were infected with the lentivirus expressing FLAG-HLA-A-HA and treated with ALLN. (*J*) The sgTRC8 or sgHRD1 Huh7 cells stably expressing US2 were infected with the lentivirus expressing HLA-A. (*K*) HEK293T cells were transfected with HLA-A-EE, HA-US2, and SPP-FOS D219/265A (M3). The IP and WCL were subjected to sodium dodecyl-sulfate polyacrylamide gel electrophoresis and immunoblotting. (*L*–*N*) Schematic representation of the HCMV US2 protein and the HCV core protein utilizing SPP. (*L*) US2 interacts with SPP and inhibits its activity, thus resulting in the TRC8-dependent degradation of MHC class I molecules. (*M*) The core protein also interacts with SPP and interferes with binding of HLA-A to SPP, thereby inducing the HRD1-dependent degradation of MHC class I molecules. (*N*) The HCV core protein and the US2 both target SPP to induce the degradation of MHC class I molecules. Both viral proteins function as immunoevasins to evade host surveillance by CD8^{+} T cells (*N*). The data are representative of two independent experiments.

100 U/mL penicillin, and 100 μg/mL streptomycin. HCV derived from the JFH-1 strain containing adaptive mutations in E2, p7, and NS2 (51) was prepared by serial passages of Huh7.5.1 cells as previously described (29).

Mice. SPPLKO mice were generated by mating SPP^{fl/fl} mice (12) and Alb-Cre transgenic mice, which express the Cre recombinase gene under the albumin promoter (52). CoreTG (53) and OT-I Tg mice (54) have been previously described. Mice (8 to 10 wk old) were gender-matched randomly assigned to experimental groups and were maintained under 12-h light/dark cycle (lights on at 08:00 AM) at 23 ± 2 °C with free access to food and water. All animal experiments were approved by the Institutional Committee of Laboratory Animal Experimentation of the Research Institute for Microbial Diseases, Osaka University (R01-11-0). All efforts were made to minimize animal suffering and to reduce the number of animals used in the experiments.

Antibodies and Reagents. The following antibodies were used: horseradish peroxidase–conjugated anti-FLAG mouse monoclonal antibody (Sigma, clone M2), anti-HA rat monoclonal antibody (Roche, clone 3F10), anti-GFP mouse monoclonal antibody (Clontech, JL-8), anti-actin mouse monoclonal antibody (Sigma, A2228), anti-HCV core mouse monoclonal antibody (Fujirebio), anti-NS5A mouse monoclonal antibody (5A27) (55), anti-EE mouse monoclonal antibody (Covance, MMS-115R), anti-EE rabbit polyclonal antibody (Covance, PRB-115C), anti-glutathione S-transferase goat polyclonal antibody (GE Healthcare, 27-4577-01), anti-human and mouse MHC class I rabbit polyclonal antibodies (Proteintech, 15240-1-AP), anti-human MHC class I monoclonal antibody (Medical & Biological Laboratories Co., Ltd. (MBL); EMR8-5), anti-human MHC class I mouse monoclonal antibody (W6/32) (Santa Cruz Biotechnology, sc-32235), anti-mouse CD8a rat monoclonal antibody (BioLegend, 53-6.7), and anti-mouse CD4 rat monoclonal antibody (BioLegend, GK1.5). The anti-SPP rabbit polyclonal antibody was generated as described previously (12). YO-01027 was synthesized by SYNthesis med chem. LY-411575 (29), cycloheximide, and ALLN were purchased from Sigma, whereas RO-0492907 and DAPT were obtained from Selleck Chemicals. Thapsigargin (Wako) and H-2K[b] OVA peptide were purchased from FUJIFILM Wako Pure Chemical Corporation and MBL, respectively. PNGase F was purchased from New England Biolabs (P0704).

Plasmids. The plasmid vectors used are summarized in *SI Appendix*, Table S1. All complementary DNAs (cDNAs) were amplified using PCR using the Tks Gflex DNA Polymerase (Takara-Bio) and cloned into the indicated plasmids using an In-Fusion HD cloning kit (Clontech). The sequences of all plasmids were confirmed using the ABI Prism 3130 genetic analyzer (Applied Biosystems).

Lentivirus Transduction. HEK293T cells (2 × 10⁶) were seeded on a 10-cm dish and incubated at 37 °C for 24 h. The cells were then transfected with pCMV-VSV-G (1.0 μg), pMDLg/pRRE (1.5 μg), pRSV-Rev (1.5 μg), and lentiviral transfer vector (FUIGW, FUIPW, or lentiCRISPR version 2; 1.5 μg) using the TransIT-LT1 Transfection Reagent (Mirus Bio) according to the manufacturer's protocol. The supernatant was collected after 24 h post-transfection and passed through a 0.45-μm filter. For transduction, target cells (2 × 10⁵) were seeded on a 6-well plate and incubated for 24 h, followed by addition of the supernatant containing the lentivirus and hexadimethrine bromide (4 μg/mL; Sigma). The samples were centrifuged at 2,500 rpm for 45 min at 32 °C, and the supernatant was replaced with a fresh medium 3 h postinfection. To generate stable cell lines, the cells infected with the lentivirus were selected using puromycin 48 h postinfection.

Immunoblotting. The cells were washed once with phosphate-buffered saline (PBS) and lysis buffer containing 20 mM Tris-HCl (pH = 7.4), 135 mM NaCl, 10% glycerol, 1% Triton X-100, and a protease inhibitor mixture (cComplete, Roche) was added. The cell lysates were incubated for 20 min on ice, and the supernatants were collected after centrifugation at 15,000 rpm for 5 min at 4 °C. The liver tissues were incubated with lysis buffer, homogenized using the BioMasher II Micro Tissue Homogenizer (DWK Life Sciences), and centrifuged at 15,000 rpm for 5 min at 4 °C. Total protein from the supernatants was quantified using a Bio-Rad Protein Assay Dye Reagent Concentrate (Bio-Rad) according to the manufacturer's protocol. Equal amounts of proteins were mixed with sodium dodecyl sulfate (SDS) gel-loading buffer (2×) containing 50 mM Tris-HCl (pH = 6.8), 4% SDS, 0.2% bromophenol blue, 10% glycerol, and 200 mM β-mercaptoethanol at 4 °C for 1 h, resolved using sodium dodecyl-sulfate polyacrylamide gel electrophoresis (NuPAGE gel, Life Technologies), transferred onto nitrocellulose membranes (iBlot, Life Technologies), blocked with PBS containing 0.05% Tween20 (PBS-T) supplemented with 5% skim milk

for 1 h, and incubated with the primary antibodies (1:2,000 dilution) at 4 °C for 24 h. After washing three times with PBS-T, the blots were incubated with secondary antibodies (1:2,000 dilution). The immune complex was visualized using the Super Signal West Femto substrate (Pierce) and detected using the LAS-4000 mini image analyzer system (FUJIFILM). The signal intensity of the proteins was calculated using the Multi Gauge software (FUJIFILM).

Immunoprecipitation. HEK293T cells (2 × 10⁶) were seeded on a 10-cm dish and incubated at 37 °C for 24 h. The cells were transfected with the plasmids via liposome-mediated transfection using polyethyleneimine (40 μL; 1 mg/mL, molecular weight, 25,000; Polysciences, Inc.). The mixtures were incubated for 20 min, added to HEK293T cells, and incubated for 48 h. The cell lysates were incubated with the antibodies at 4 °C for 24 h and with Protein G Sepharose 4B (GE Healthcare) at 4 °C for 1 h. The beads were washed five times with the lysis buffer, boiled at 60 °C for 20 min with the sample buffer, and subjected to immunoblotting.

Generation of SPP, TRC8, and HRD1-Knockout Cell Lines. To construct the single-guide RNA targeting the SPP, TRC8, and HRD1, the targeting sequences were designed using three different sequences for each gene as previously described (56), synthesized using DNA oligos (Eurofins Genetics), and cloned into the lentiCRISPR version 2 (Addgene, no. 52961) digested by BmsBI (New England Biolab). The following target sequences were used: HRD1 5′-GGAAGACAAGGACAAAGGCC-3′, 5′-GTGAAGAGTGCAACAAAG-CG-3′, and 5′-GAAAGAGCCAGGAGATGTTG-3′; TRC8 5′-GCGCCGCCCAGA-CCTGCTGA-3′, 5′-GCTTTGGCTGGAATCCGGGT-3′, and 5′-GGTGCGGATGGC-CCATCAGC-3′; and SPP 5′-GCCCTCAGCGATCCGCATAA-3′, 5′-CACGCCCGAGGG-CATCGCGC-3′, and 5′-GTCCATGTATTTCTTCGTGC-3′. Lentiviruses expressing three kinds of target sequences per gene were mixed, introduced into the target cells, and maintained in a culture medium supplemented with 1 μg/mL puromycin for 3 wk.

Flow Cytometry. Cells (2 × 10⁵) were collected and resuspended in fluorescence-activated cell sorting (FACS) buffer containing 2% FBS in PBS and incubated with the anti-MHC class I antibody (W6/32; Santa Cruz Biotechnology, sc-32235) at 4 °C for 30 min. After washing twice with the FACS buffer, the cells were further incubated at 4 °C for 30 min with the AF488-conjugated anti-mouse antibody and washed with the FACS buffer. The surface expression of MHC I was measured using FACSAria (BD Immunocytometry System) and analyzed using FlowJo (FlowJo LLC).

Quantitative RT-PCR. Total RNA was extracted from the liver lysates using ISOGEN II (Nippon Gene) according to the manufacturer's protocol. Subsequently, cDNAs were synthesized using a high-capacity RNA-to-cDNA kit (Applied Biosystems) according to the manufacturer's instructions and those of HLA-A, IFNα1, IFNβ1, IL6, TNFα, IP10, CCL5, and β-actin were quantified using Fast SYBR Green Master Mix (Thermo Fisher Scientific) and ViiA7 RT-PCR system (Thermo Fisher Scientific). The following primers were used: HLA-A, 5′-GGCCCTGACCCAGACCTG-3′ and 5′-GCACGAACTGCGTGTCGTC-3′; IFNα1, 5′-AGCCTTGACACTCCTGGTACAAATG-3′ and 5′-TGGGTCAGCTCACTCAGGACA-3′; IFNβ1, 5′-ACACCAGCCTGGCTTCCATC-3′ and 5′-TTGGAGCTGGAGCTGCTTATAGTTG-3′; IL6, 5′-CCACTTCACAAGTCGGAG-GCTTA-3′ and 5′-GCAAGTGCATCATCGTTGTTCATAC-3′; TNFα, 5′-CAGGAGGGA-GAACAGAAACTCCA-3′ and 5′-CCTGGTTGGCTGCTTGCTT-3′; IP10, 5′-ACACCA-GCCTGGCTTCCATC-3′ and 5′-TTGGAGCTGGAGCTGCTTATAGTTG-3′; CCL5, 5′-AGATCTCTGCAGCTGCCCTCA-3′ and 5′-GGAGCACTTGCTGCTGGTGTAG-3′; and β-actin, 5′-TTGCTGACAGGATGCAGAAG-3′ and 5′-GTACTTGCGCTCAGGAGGAG-3′. The relative mRNA expression was calculated using the delta-delta Ct method, with β-actin as the internal control.

Luciferase Assay. Cells were seeded on a 24-well plate and incubated at 37 °C for 24 h. pERAI-Luc, pRL-SV40 and the HCV core, HLA-A, Prolactin, HO-1, or XBP1u were transfected into the cells using TransIT-LT1 (Mirus Bio) according to the manufacturer's protocol. The cells were incubated for 24 h after transfection, and luciferase activity was detected using the Dual-Luciferase Reporter Assay System (Promega) according to the manufacturer's protocol.

In Vitro Antigen Presentation Assay. CD8⁺ T cells derived from the spleen of OT-I transgenic mice were isolated using a CD8⁺ T cell Isolation kit (Miltenyi Biotec). MEFs expressing GFP alone or GFP and the core protein were identified using a cell sorter (SONY SH800S). Hepatocytes derived from the WT or CoreTg were isolated using a perfusion method described previously (57). Briefly, the mice were euthanized by inhalation of isoflurane anesthesia, and

livers were perfused using Hank's balanced salt solution containing 0.5 mM egtazic acid followed by perfusion using a liver digest medium (Thermo Fisher). Isolated hepatocytes were purified using a Percoll gradient. MEFs or hepatocytes (2×10^4) were seeded on a 96-well plate, incubated for 24 h, and further incubated with the H-2K^b OVA peptide (1.0 nM; TS-50001-P, MBL Life Science) for 7 h. The cells were washed once with PBS and fixed with 0.01% glutaraldehyde in PBS for 30 s. The reaction was quenched by adding 0.2 M glycine in PBS, and the cells were washed twice with PBS and once with Roswell Park Memorial Institute-1640 supplemented with 10% FBS, 2 mM L-Glutamine (Gibco), 1 mM sodium pyruvate (Wako), 100 U/mL penicillin, and 100 μg/mL streptomycin and cocultured with CD8$^+$ T cells. Culture supernatants were collected after 72 h, and IFN-γ production was quantified.

Enzyme-Linked Immunosorbent Assay. IFN-γ in culture supernatants of mouse CD8$^+$ T cells were quantified using enzyme-linked immunosorbent assay MAX Deluxe Set Mouse IFN-γ (BioLegend) according to the manufacturer's protocol.

Preparation of Human Liver Tissues. Liver samples were obtained from 18 patients with HCC who underwent curative liver resection at the Cancer Institute Hospital of Japanese Foundation for Cancer Research. The study protocol adhered to the ethical guidelines of human clinical research established by the Japanese Ministry of Health, Labor and Welfare and was approved by the ethics committees of the participating facilities (NCGM-A-000227, Japanese Foundation for Cancer Research under Clinical Research Number 2017-1118). Written informed consent was obtained from all patients during enrollment.

Freshly frozen tissue samples from normal adjacent tissues were obtained from patients with liver metastasis of colon cancer, chronic hepatitis C infection, SVR, or nonalcoholic fatty liver disease (*SI Appendix*, Table S2). The liver tissues were added to the lysis buffer, homogenized using a BioMasher II Micro Tissue Homogenizer (DWK Life Sciences), and centrifuged at 15,000 rpm for 5 min at 4 °C. The total protein concentration of the supernatants was quantified using a Bio-Rad Protein Assay Dye Reagent Concentrate (Bio-Rad) according to the manufacturer's protocol, and equal amounts of proteins were subjected to immunoblotting.

Histological Analysis. Liver tissues were fixed with 10% formalin, impregnated with 30% sucrose, and frozen with the Tissue-Tek OCT compound (Sakura Finetek). Next, 10-μm–thick tissue sections were prepared and stained with hematoxylin and eosin. Additionally, Oil red O staining was performed on frozen sections that were washed once with running tap water for 5 min, rinsed with 60% isopropanol for 1 min, stained with the staining solution for 15 min, rinsed with 60% isopropanol, and subjected to light staining of the nuclei with hematoxylin for 15 s. All sections were observed under a microscope (Olympus).

Homology Modeling of the Core and US2 Proteins. Structural information for the HCV core protein (JFH1 strain) was obtained from the Protein Data Bank (PDB ID code: 2LIF) and was used as a template to model the core protein (J1 strain) and US2 protein, and their sequences were aligned using HHpred. Their structural models were built using the MODELER program, and the images were constructed using the open-source PyMOL Molecular Graphics System version 1.8.6.0.

Quantification and Statistical Analysis. All statistical analyses were conducted using the GraphPad Prism version 8.4.3 (GraphPad Software). Student's *t* test was used to determine significant differences, and the statistical details of the experiments are indicated in the figure legends.

Data Availability. All study data are included in the article and/or supporting information.

1. B. Maasoumy, H. Wedemeyer, Natural history of acute and chronic hepatitis C. *Best Pract. Res. Clin. Gastroenterol.* **26**, 401–412 (2012).
2. A. Galossi, R. Guarisco, L. Bellis, C. Puoti, Extrahepatic manifestations of chronic HCV infection. *J. Gastrointestin. Liver Dis.* **16**, 65–73 (2007).
3. S. L. Chen, T. R. Morgan, The natural history of hepatitis C virus (HCV) infection. *Int. J. Med. Sci.* **3**, 47–52 (2006).
4. M. H. Heim, R. Thimme, Innate and adaptive immune responses in HCV infections. *J. Hepatol.* **61** (suppl.(1), S14–S25 (2014).
5. A. B. Jazwinski, A. J. Muir, Direct-acting antiviral medications for chronic hepatitis C virus infection. *Gastroenterol. Hepatol. (N. Y.)* **7**, 154–162 (2011).
6. F. Conti et al., Early occurrence and recurrence of hepatocellular carcinoma in HCV-related cirrhosis treated with direct-acting antivirals. *J. Hepatol.* **65**, 727–733 (2016).
7. J. Hengst et al., Nonreversible MAIT cell-dysfunction in chronic hepatitis C virus infection despite successful interferon-free therapy. *Eur. J. Immunol.* **46**, 2204–2210 (2016).
8. B. Langhans et al., Increased peripheral CD4$^+$ regulatory T cells persist after successful direct-acting antiviral treatment of chronic hepatitis C. *J. Hepatol.* **66**, 888–896 (2017).
9. R. Bartenschlager, V. Lohmann, F. Penin, The molecular and structural basis of advanced antiviral therapy for hepatitis C virus infection. *Nat. Rev. Microbiol.* **11**, 482–496 (2013).
10. Y. Mori, K. Moriishi, Y. Matsuura, Hepatitis C virus core protein: Its coordinate roles with PA28gamma in metabolic abnormality and carcinogenicity in the liver. *Int. J. Biochem. Cell Biol.* **40**, 1437–1442 (2008).
11. R. M. Gemmill et al., The hereditary renal cell carcinoma 3;8 translocation fuses FHIT to a patched-related gene, TRC8. *Proc. Natl. Acad. Sci. U.S.A.* **95**, 9572–9577 (1998).
12. S. Aizawa et al., TRC8-dependent degradation of hepatitis C virus immature core protein regulates viral propagation and pathogenesis. *Nat. Commun.* **7**, 11379 (2016).
13. M. K. Lemberg, F. A. Bland, A. Weihofen, V. M. Braud, B. Martoglio, Intramembrane proteolysis of signal peptides: An essential step in the generation of HLA-E epitopes. *J. Immunol.* **167**, 6441–6446 (2001).
14. J. M. Boname et al., Cleavage by signal peptide peptidase is required for the degradation of selected tail-anchored proteins. *J. Cell Biol.* **205**, 847–862 (2014).
15. C.-Y. Chen et al., Signal peptide peptidase functions in ERAD to cleave the unfolded protein response regulator XBP1u. *EMBO J.* **33**, 2492–2506 (2014).
16. B. Martoglio, R. Graf, B. Dobberstein, Signal peptide fragments of preprolactin and HIV-1 p-gp160 interact with calmodulin. *EMBO J.* **16**, 6636–6645 (1997).
17. J. Levitskaya et al., Inhibition of antigen processing by the internal repeat region of the Epstein-Barr virus nuclear antigen-1. *Nature* **375**, 685–688 (1995).
18. N. P. Dantuma, S. Heessen, K. Lindsten, M. Jellne, M. G. Masucci, Inhibition of proteasomal degradation by the gly-Ala repeat of Epstein-Barr virus is influenced by the length of the repeat and the strength of the degradation signal. *Proc. Natl. Acad. Sci. U.S.A.* **97**, 8381–8385 (2000).
19. K. Früh et al., A viral inhibitor of peptide transporters for antigen presentation. *Nature* **375**, 415–418 (1995).
20. K. Ahn et al., The ER-luminal domain of the HCMV glycoprotein US6 inhibits peptide translocation by TAP. *Immunity* **6**, 613–621 (1997).
21. P. J. Lehner, J. T. Karttunen, G. W. Wilkinson, P. Cresswell, The human cytomegalovirus US6 glycoprotein inhibits transporter associated with antigen processing-dependent peptide translocation. *Proc. Natl. Acad. Sci. U.S.A.* **94**, 6904–6909 (1997).
22. E. M. Bennett, J. R. Bennink, J. W. Yewdell, F. M. Brodsky, Cutting edge: Adenovirus E19 has two mechanisms for affecting class I MHC expression. *J. Immunol.* **162**, 5049–5052 (1999).
23. J. F. Roeth, M. Williams, M. R. Kasper, T. M. Filzen, K. L. Collins, HIV-1 Nef disrupts MHC-I trafficking by recruiting AP-1 to the MHC-I cytoplasmic tail. *J. Cell Biol.* **167**, 903–913 (2004).
24. J. R. Francica et al., Steric shielding of surface epitopes and impaired immune recognition induced by the ebola virus glycoprotein. *PLoS Pathog.* **6**, e1001098 (2010).
25. H. R. Stagg et al., The TRC8 E3 ligase ubiquitinates MHC class I molecules before dislocation from the ER. *J. Cell Biol.* **186**, 685–692 (2009).
26. J. M. Boname, P. G. Stevenson, MHC class I ubiquitination by a viral PHD/LAP finger protein. *Immunity* **15**, 627–636 (2001).
27. X. Wang et al., Ubiquitination of serine, threonine, or lysine residues on the cytoplasmic tail can induce ERAD of MHC-I by viral E3 ligase mK3. *J. Cell Biol.* **177**, 613–624 (2007).
28. D. J. H. van den Boomen et al., TMEM129 is a Derlin-1 associated ERAD E3 ligase essential for virus-induced degradation of MHC-I. *Proc. Natl. Acad. Sci. U.S.A.* **111**, 11425–11430 (2014).
29. J. Hirano et al., Characterization of SPP inhibitors suppressing propagation of HCV and protozoa. *Proc. Natl. Acad. Sci. U.S.A.* **114**, E10782–E10791 (2017).
30. E. A. Hughes, C. Hammond, P. Cresswell, Misfolded major histocompatibility complex class I heavy chains are translocated into the cytoplasm and degraded by the proteasome. *Proc. Natl. Acad. Sci. U.S.A.* **94**, 1896–1901 (1997).
31. M. L. Burr et al., HRD1 and UBE2J1 target misfolded MHC class I heavy chains for endoplasmic reticulum-associated degradation. *Proc. Natl. Acad. Sci. U.S.A.* **108**, 2034–2039 (2011).

Hirano et al.
Hepatitis C virus modulates signal peptide peptidase to alter host protein processing

PNAS | 11 of 12
https://doi.org/10.1073/pnas.2026184118

32. R. T. Timms *et al*., Genetic dissection of mammalian ERAD through comparative haploid and CRISPR forward genetic screens. *Nat. Commun.* **7**, 11786 (2016).

33. T. Tanaka *et al*., Hallmarks of hepatitis C virus in equine hepacivirus. *J. Virol.* **88**, 13352–13366 (2014).

34. J. Loureiro *et al*., Signal peptide peptidase is required for dislocation from the endoplasmic reticulum. *Nature* **441**, 894–897 (2006).

35. K. M. Paulsson *et al*., Distinct differences in association of MHC class I with endoplasmic reticulum proteins in wild-type, and beta 2-microglobulin- and TAP-deficient cell lines. *Int. Immunol.* **13**, 1063–1073 (2001).

36. L. Mancino, S. M. Rizvi, P. E. Lapinski, M. Raghavan, Calreticulin recognizes misfolded HLA-A2 heavy chains. *Proc. Natl. Acad. Sci. U.S.A.* **99**, 5931–5936 (2002).

37. Y. Zhang, E. Baig, D. B. Williams, Functions of ERp57 in the folding and assembly of major histocompatibility complex class I molecules. *J. Biol. Chem.* **281**, 14622–14631 (2006).

38. J. A. Lindquist, O. N. Jensen, M. Mann, G. J. Hämmerling, ER-60, a chaperone with thiol-dependent reductase activity involved in MHC class I assembly. *EMBO J.* **17**, 2186–2195 (1998).

39. E. Rufer, R. M. Leonhardt, M. R. Knittler, Molecular architecture of the TAP-associated MHC class I peptide-loading complex. *J. Immunol.* **179**, 5717–5727 (2007).

40. M. L. Burr *et al*., MHC class I molecules are preferentially ubiquitinated on endoplasmic reticulum luminal residues during HRD1 ubiquitin E3 ligase-mediated dislocation. *Proc. Natl. Acad. Sci. U.S.A.* **110**, 14290–14295 (2013).

41. A. Cauli *et al*., [The role of HLA-27 molecules in the pathogenesis of ankylosing spondylitis]. *Reumatismo* **54**, 266–271 (2002).

42. R. A. Colbert, T. M. Tran, G. Layh-Schmitt, HLA-B27 misfolding and ankylosing spondylitis. *Mol. Immunol.* **57**, 44–51 (2014).

43. A. Waheed *et al*., Hereditary hemochromatosis: Effects of C282Y and H63D mutations on association with beta2-microglobulin, intracellular processing, and cell surface expression of the HFE protein in COS-7 cells. *Proc. Natl. Acad. Sci. U.S.A.* **94**, 12384–12389 (1997).

44. X. Shi *et al*., Bunyamwera orthobunyavirus glycoprotein precursor is processed by cellular signal peptidase and signal peptide peptidase. *Proc. Natl. Acad. Sci. U.S.A.* **113**, 8825–8830 (2016).

45. S. J. Allen *et al*., Binding of HSV-1 glycoprotein K (gK) to signal peptide peptidase (SPP) is required for virus infectivity. *PLoS One* **9**, e85360 (2014).

46. S. Wang, H. Ghiasi, Absence of signal peptide peptidase, an essential herpes simplex virus 1 glycoprotein K binding partner, reduces virus infectivity in vivo. *J. Virol.* **93**, e01309-19 (2019).

47. S.-R. Lee, B. Nanduri, G. T. Pharr, J. V. Stokes, L. M. Pinchuk, Bovine viral diarrhea virus infection affects the expression of proteins related to professional antigen presentation in bovine monocytes. *Biochim. Biophys. Acta* **1794**, 14–22 (2009).

48. C. Burrells *et al*., Lymphocyte subpopulations in the blood of sheep persistently infected with border disease virus. *Clin. Exp. Immunol.* **76**, 446–451 (1989).

49. L. L. Lanier, NK cell recognition. *Annu. Rev. Immunol.* **23**, 225–274 (2005).

50. P. Rodrigues *et al*., Comparative study between Hfe-/- and beta2m-/- mice: Progression with age of iron status and liver pathology. *Int. J. Exp. Pathol.* **87**, 317–324 (2006).

51. R. S. Russell *et al*., Advantages of a single-cycle production assay to study cell culture-adaptive mutations of hepatitis C virus. *Proc. Natl. Acad. Sci. U.S.A.* **105**, 4370–4375 (2008).

52. T. Kodama *et al*., Increases in p53 expression induce CTGF synthesis by mouse and human hepatocytes and result in liver fibrosis in mice. *J. Clin. Invest.* **121**, 3343–3356 (2011).

53. K. Moriya *et al*., Hepatitis C virus core protein induces hepatic steatosis in transgenic mice. *J. Gen. Virol.* **78**, 1527–1531 (1997).

54. Y. Lee *et al*., p62 plays a specific role in interferon-γ-induced presentation of a toxoplasma vacuolar antigen. *Cell Rep.* **13**, 223–233 (2015).

55. K. Okamoto *et al*., Intramembrane processing by signal peptide peptidase regulates the membrane localization of hepatitis C virus core protein and viral propagation. *J. Virol.* **82**, 8349–8361 (2008).

56. N. E. Sanjana, O. Shalem, F. Zhang, Improved vectors and genome-wide libraries for CRISPR screening. *Nat. Methods* **11**, 783–784 (2014).

57. Y. Itoh *et al*., Salt-inducible kinase 3 signaling is important for the gluconeogenic programs in mouse hepatocytes. *J. Biol. Chem.* **290**, 17879–17893 (2015).

Hirano et al.
Hepatitis C virus modulates signal peptide peptidase to alter host protein processing